Experimental study of fs-laser induced sub-100-nm periodic surface structures on titanium

Chandra S.R. Nathala,[1,2] Ali Ajami,[1] Andrey A. Ionin,[3] Sergey I. Kudryashov,[3,4] Sergey V Makarov,[3,5] Thomas Ganz,[2] Andreas Assion,[2] Wolfgang Husinsky[1,*]

[1]*IAP, Vienna University of Technology, Wiedner Hauptstrasse 8-10, 1040 Vienna, Austria*
[2]*Femtolasers Productions GmbH, Fernkorngasse10, 1100 Vienna, Austria*
[3]*P N Lebedev Physical Institute RAS, Leninskiy prospect 53, 119991 Moscow, Russia*
[4]*National Research Nuclear University MEPhI (Moscow Engineering Physics Institute), Kashirskoe shosse 31, 115409 Moscow, Russia*
[5]*ITMO University, Kronverkskiy prospect 49, 197101, St. Petersburg, Russia*
[*]*husinsky@iap.tuwien.ac.at*

Abstract: In this work the formation of laser-induced periodic surface structures (LIPSS) on a titanium surface upon irradiation by linearly polarized femtosecond (fs) laser pulses with a repetition rate of 1 kHz in air environment was studied experimentally. In particular, the dependence of high-spatial-frequency-LIPSS (HSFL) characteristics on various laser parameters: fluence, pulse number, wavelength (800 nm and 400 nm), pulse duration (10 fs – 550 fs), and polarization was studied in detail. In comparison with low-spatial-frequency-LIPSS (LSFL), the HSFL emerge at a much lower fluence with orientation perpendicular to the ridges of the LSFL. It was observed that these two types of LIPSS demonstrate different fluence, shot number and wavelength dependencies, which suggest their origin is different. Therefore, the HSFL formation mechanism cannot be described by the widely accepted interference model developed for describing LSFL formation.

OCIS codes: (140.3390) Laser materials processing; (140.7090) Ultrafast lasers; (310.6628) Subwavelength structures, nanostructures.

References and links

1. S. Bashir, M. Shahid Rafique, and W. Husinsky, "Femtosecond laser-induced subwavelength ripples on Al, Si, CaF2 and CR-39," Nucl. Instrum. Methods Phys. Res. B **275**, 1–6 (2012).
2. J. Bonse, A. Rosenfeld, and J. Krüger, "On the role of surface plasmon polaritons in the formation of laser-induced periodic surface structures upon irradiation of silicon by femtosecond-laser pulses," J. Appl. Phys. **106**(10), 104910 (2009).
3. A. Borowiec and H. K. Haugen, "Subwavelength ripple formation on the surfaces of compound semiconductors irradiated with femtosecond laser pulses," Appl. Phys. Lett. **82**(25), 4462–4464 (2003).
4. E. V. Golosov, A. A. Ionin, Y. R. Kolobov, S. I. Kudryashov, A. E. Ligachev, S. V. Makarov, Y. N. Novoselov, L. V. Seleznev, D. V. Sinitsyn, and A. R. Sharipov, "Near-threshold femtosecond laser fabrication of one-dimensional subwavelength nanogratings on a graphite surface," Phys. Rev. B **83**(11), 115426 (2011).
5. M. Huang, F. Zhao, Y. Cheng, N. Xu, and Z. Xu, "Origin of laser-induced near-subwavelength ripples: interference between surface plasmons and incident laser," ACS Nano **3**(12), 4062–4070 (2009).
6. Q. Wu, Y. Ma, R. Fang, Y. Liao, Q. Yu, X. Chen, and K. Wang, "Femtosecond laser-induced periodic surface structure on diamond film," Appl. Phys. Lett. **82**(11), 1703–1705 (2003).
7. J. E. Sipe, J. F. Young, J. S. Preston, and H. M. van Driel, "Laser-induced periodic surface structure. I. Theory," Phys. Rev. B **27**(2), 1141–1154 (1983).
8. S. A. Akhmanov, V. I. Emel'yanov, N. I. Koroteev, and V. N. Seminogov, "Interaction of powerful laser radiation with the surfaces of semiconductors and metals: nonlinear optical effects and nonlinear optical diagnostics," Sov. Phys. Usp. **28**(12), 1084–1124 (1985).
9. J. Z. P. Skolski, G. R. B. E. Römer, A. J. Huis in 't Veld, V. S. Mitko, J. V. Obona, V. Ocelik, and J. T. M. D. Hosson, "Modeling of laser induced periodic surface structures," J. Laser Micro/nano. Eng. **5**(3), 263–268 (2010).
10. A. A. Ionin, S. I. Kudryashov, A. E. Ligachev, S. V. Makarov, L. V. Seleznev, and D. V. Sinitsyn, "Nanoscale cavitation instability of the surface melt along the grooves of one-dimensional nanorelief gratings on an aluminum surface," J. Exp. Theor. Phys. Lett. **94**(4), 266–269 (2011).

#229000 - $15.00 USD Received 4 Dec 2014; revised 30 Jan 2015; accepted 2 Feb 2015; published 25 Feb 2015

11. A. A. Ionin, S. I. Kudryashov, S. V. Makarov, L. V. Seleznev, D. V. Sinitsyn, A. E. Ligachev, E. V. Golosov, and Yu. R. Kolobov, "Sub-100 nanometer transverse gratings written by femtosecond laser pulses on a titanium surface," Laser Phys. Lett. **10**(5), 056004 (2013).
12. J. Bonse, S. Höhm, A. Rosenfeld, and J. Krüger, "Sub-100-nm laser-induced periodic surface structures upon irradiation of titanium by Ti:sapphire femtosecond laser pulses in air," Appl. Phys., A Mater. Sci. Process. **110**(3), 547–551 (2013).
13. J. Z. P. Skolski, G. R. B. E. Römer, J. Vincenc Obona, and A. J. Huis in 't Veld, "Modeling laser-induced periodic surface structures: Finite-difference time-domain feedback simulations," J. Appl. Phys. **115**(10), 103102 (2014).
14. C. Guo, G. Rodriguez, A. Lobad, and A. J. Taylor, "Structural phase transition of aluminum induced by electronic excitation," Phys. Rev. Lett. **84**(19), 4493–4496 (2000).
15. E. V. Golosov, A. A. Ionin, Y. R. Kolobov, S. I. Kudryashov, A. E. Ligachev, S. V. Makarov, Y. N. Novoselov, L. V. Seleznev, and D. V. Sinitsyn, "Formation of periodic nanostructures on aluminum surface by femtosecond laser pulses," Nanotechnol. Russ. **6**(3-4), 237–243 (2011).
16. X.-F. Li, C.-Y. Zhang, H. Li, Q.-F. Dai, S. Lan, and S.-L. Tie, "Formation of 100-nm periodic structures on a titanium surface by exploiting the oxidation and third harmonic generation induced by femtosecond laser pulses," Opt. Express **22**(23), 28086–28099 (2014).
17. K. Bazaka, R. J. Crawford, and E. P. Ivanova, "Do bacteria differentiate between degrees of nanoscale surface roughness?" Biotechnol. J. **6**(9), 1103–1114 (2011).
18. J. M. Liu, "Simple technique for measurements of pulsed Gaussian-beam spot sizes," Opt. Lett. **7**(5), 196–198 (1982).
19. M. Ye and C. P. Grigoropoulos, "Time-of-flight and emission spectroscopy study of femtosecond laser ablation of titanium," J. Appl. Phys. **89**(9), 5183–5190 (2001).
20. J. Byskov-Nielsen, J.-M. Savolainen, M. Christensen, and P. Balling, "Ultra-short pulse laser ablation of metals: threshold fluence, incubation coefficient and ablation rates," Appl. Phys., A Mater. Sci. Process. **101**(1), 97–101 (2010).
21. N. Yasumaru, K. Miyazaki, and J. Kiuchi, "Fluence dependence of femtosecond-laser-induced nanostructure formed on TiN and CrN," Appl. Phys., A Mater. Sci. Process. **81**(5), 933–937 (2005).
22. M. Okamuro, M. Hashida, Y. Miyasaka, Y. Ikuta, S. Tokita, and S. Sakabe, "Laser fluence dependence of periodic grating structures formed on metal surfaces under femtosecond laser pulse irradiation," Phys. Rev. B **82**(16), 165417 (2010).
23. A. A. Ionin, S. I. Kudryashov, S. V. Makarov, A. A. Rudenko, L. V. Seleznev, D. V. Sinitsyn, and V. I. Emel'yanov, "Nonlinear optical dynamics during femtosecond laser nanostructuring of a silicon surface," Laser Phys. Lett. **12**(2), 025902 (2015).
24. J. Bonse and J. Krüger, "Pulse number dependence of laser-induced periodic surface structures for femtosecond laser irradiation of silicon," J. Appl. Phys. **108**(3), 034903 (2010).
25. M. Huang, F. Zhao, Y. Cheng, N. Xu, and Z. Xu, "Large area uniform nanostructures fabricated by direct femtosecond laser ablation," Opt. Express **16**(23), 19354–19365 (2008).
26. O. Varlamova, F. Costache, J. Reif, and M. Bestehorn, "Self-organized pattern formation upon femtosecond laser ablation by circularly polarized light," Appl. Surf. Sci. **252**(13), 4702–4706 (2006).
27. T. Tomita, K. Kinoshita, S. Matsuo, and S. Hashimoto, "Effect of surface roughening on femtosecond laser-induced ripple structures," Appl. Phys. Lett. **90**(15), 153115 (2007).
28. I. Kudryashov, (private communication, unpublished results).
29. I. A. Artyukov, D. A. Zayarniy, A. A. Ionin, S. I. Kudryashov, S. V. Makarov, and P. N. Saltuganov, "Relaxation phenomena in electronic and lattice subsystems on iron surface during its ablation by ultrashort laser pulses," JETP Lett. **99**(1), 51–55 (2014).
30. E. V. Barmina, A. A. Serkov, E. Stratakis, C. Fotakis, V. N. Stolyarov, I. N. Stolyarov, and G. A. Shafeev, "Nano-textured W shows improvement of thermionic emission properties," Appl. Phys., A Mater. Sci. Process. **106**(1), 1–4 (2012).
31. S. Höhm, M. Herzlieb, A. Rosenfeld, J. Krüger, and J. Bonse, "Femtosecond laser-induced periodic surface structures on silicon upon polarization controlled two-color double-pulse irradiation," Opt. Express **23**(1), 61–71 (2015).
32. E. V. Golosov, A. A. Ionin, Y. R. Kolobov, S. I. Kudryashov, A. E. Ligachev, Y. N. Novoselov, L. V. Seleznev, and D. V. Sinitsyn, "Ultrafast changes in the optical properties of a titanium surface and femtosecond laser writing of one-dimensional quasi-periodic nanogratings of its relief," Sov. Phys. JETP **113**(1), 14–26 (2011).
33. J.-W. Yao, C.-Y. Zhang, H.-Y. Liu, Q.-F. Dai, L.-J. Wu, S. Lan, A. V. Gopal, V. A. Trofimov, and T. M. Lysak, "High spatial frequency periodic structures induced on metal surface by femtosecond laser pulses," Opt. Express **20**(2), 905–911 (2012).
34. H. Raether, "Surface plasmons on smooth and rough surfaces and on gratings", Springer, Berlin, 1988, Chapter 1.
35. A. A. Ionin, S. I. Kudryashov, L. V. Seleznev, D. V. Sinitsyn, A. F. Bunkin, V. N. Lednev, and S. M. Pershin, "Thermal melting and ablation of silicon surface by femtosecond laser radiation," Sov. Phys. JETP-USSR **116**, 347–362 (2013).
36. J.-M. Savolainen, M. S. Christensen, and P. Balling, "Material swelling as the first step in the ablation of metals by ultrashort laser pulses," Phys. Rev. B **84**(19), 193410 (2011).
37. A. Y. Vorobyev and C. Guo, "Femtosecond laser structuring of titanium implants," Appl. Surf. Sci. **253**(17), 7272–7280 (2007).

#229000 - $15.00 USD Received 4 Dec 2014; revised 30 Jan 2015; accepted 2 Feb 2015; published 25 Feb 2015

38. P. B. Johnson, P. W. Gilberd, Y. Morrison, and C. R. Varoy, "Gas-bubble ordering in nanoporous surface formation in helium-implanted metals," Mod. Phys. Lett. B **15**(28n29), 1391–1401 (2001).
39. S. I. Ashitkov, N. A. Inogamov, V. V. Zhakhovskii, Y. N. Emirov, M. B. Agranat, I. I. Oleinik, S. I. Anisimov, and V. E. Fortov, "Formation of nanocavities in the surface layer of an aluminum target irradiated by a femtosecond laser pulse," JETP Lett. **95**(4), 176–181 (2012).
40. C. Wu and L. Zhigilei, "Microscopic mechanisms of laser spallation and ablation of metal targets from large-scale molecular dynamics simulations," Appl. Phys., A Mater. Sci. Process. **114**(1), 11–32 (2014).

1. Introduction

In the last decade IR fs-laser pulses have been applied successfully for the formation of surface gratings (or ripples) in air with an orientation perpendicular to the laser polarization and periods in the range $\lambda/20 - \lambda$ [1–6], widely referred to as laser-induced periodic surface structures (LIPSS). Their origin is supposed to be related to the excitation of surface plasmon-polaritons (SPP) [7–9], which are transverse magnetic (TM) waves [2,4,5]. However, recently observed high-spatial-frequency-LIPSS (HSFL) on metals with orientation parallel to the laser polarization [10–12] cannot be explained via SPP excitation, existing at the negative real part of material dielectric function, or by other surface electromagnetic modes existing at the positive real part of the material dielectric function [7,13]. In fact for example, the real part of the dielectric function of aluminum (Al) is strongly negative in the vis-IR range [14,15], supporting only SPP (i.e. TM-modes) with wavelength values close to the exciting laser wavelengths. Therefore, it was supposed that the origin of HSFL formation lies in the formation of cavitation instabilities in the melted surface layer [10,11]. Recently, principally different, original and rather sophisticated HSFL generation mechanism has been proposed [16], considering multi-shot minor fs-laser oxidation of titanium (Ti) surface and third-harmonic generation at the oxidized surface to explain HSFL appearance with periods down to one tenth of the employed fs-laser wavelengths within the common interference model [7,8].

Another problem in understanding the origin of HSFL with orientation parallel to the laser polarization is their distribution on the surface. Some authors reported homogeneously distributed structures [12], but in the other studies it was found that the HSFL grow along stripes separated by distances exactly equal to the low-spatial-frequency-LIPSS (LSFL) periods [10, 11]. Since these two types of nanoripples have been studied separately, it is still unclear whether they are connected or independent of each other.

The aim of this work is to reveal common rules for femtosecond laser-induced sub-100-nm HSFL on titanium surface in air and resolve any ambiguities in the known literature data concerning this type of structures. We choose titanium due to its high importance in biological and medical applications, where control of morphology at nanoscale is required [17].

2. Experimental procedure

The femtosecond laser used in these experiments (Femtolasers, Femtopower Compact PRO) generates pulses centered at $\lambda \approx 800$ nm (the spectral full width at half maximum > 40 nm) with maximum energy $E = 1$ mJ/pulse of $t = 30$ fs duration at repetition rate of $u = 1$ kHz. The samples used in these experiments are mechanically polished 0.89-mm thick commercial titanium foil (metal basis, 99.7% purity, Alfa Aesar GmbH) and mirror-like titanium films with a thickness of 200 nm deposited by magnetron sputtering technique on a Borosilicate glass substrate.

The samples were irradiated in stationary and scanning modes with different fluences, number of pulses, pulse durations, wavelength and polarization. In scanning mode, the number of pulses N is varied by changing the scanning speed V, following the relation $N = 2w_0u/V$, where w_0 is the Gaussian beam radius at the focusing plane. The pulses were focused by one-inch 90° off-axis parabolic mirrors, on the target mounted on a XYZ motorized stage perpendicular to the focusing beam. Two focusing mirrors of focal length 50 mm and 150 mm were used for the exposures. A Gaussian beam radius of w_0 ($1/e^2$) = 11.0 mm and 22.0 mm was determined at the processing plane for 50 mm and 150 mm focusing mirrors

#229000 - $15.00 USD Received 4 Dec 2014; revised 30 Jan 2015; accepted 2 Feb 2015; published 25 Feb 2015

respectively, using the method proposed by Liu [18]. The pulse duration (τ) is varied by changing the dispersive path length of the compressor in the amplifier. The 10 fs duration pulses (the spectral full width at tenth of maximum > 300 nm) used in the experiments are generated by a hollow-core-fiber and compressor unit (Kaleidoscope, Femtolasers). The number of pulses (spaced 1 ms apart) are extracted by controlling the internal Pockels cell of the amplifier. The energy is varied by a half-wave plate and a polarizer unit followed by a neutral density (ND) filter placed before the compressor in the amplifier. Before each exposure, the pulse energy (E) is measured after the off-axis mirror, by a pyroelectric detector (J-10MB-LE, Coherent) and an energy meter (LabMax-TOP, Coherent). Standard deviation of pulse-to-pulse energy stability was determined to be 1.3%, but the peak-to-peak pulse energy variation over 500 pulses was about 7.5%. The pulse duration was measured by a homemade background free autocorrelator and commercially available autocorrelator (Femtometer, Femtolasers). To study the polarization dependence, a half-wave plate was installed before the focusing mirror. In the scanning mode, the target is moved in the focal plane at a constant velocity in the range of 0.2 mm/s to 2.5 mm/s, while the laser was continuously running at the fixed repetition rate of 1 kHz. The $\lambda \approx 400$ nm beam used for exposures was generated by frequency doubling of 800-nm pulses using a Beta Barium Borate (BBO) crystal and subsequently filtered from fundamental by using two dielectric mirrors having high reflectivity for 400-nm light and high transmission for 800-nm light.

The irradiated samples were examined using a scanning electron microscope (SEM, Quanta 200F, FEI) and atomic-force-microscope (AFM, Cypher, Asylum Research). SEM images were analyzed using ImageJ software. The periodicity of ripples was determined by 1D Fourier transform of SEM micrographs in the centre of irradiated regions where the fluence of the Gaussian distributed laser beam is maximum ($F = 2E/\pi w_0^2$). The local fluence values (at a distance r from the center of irradiation) in the data presented in Sec. 3.4 and Sec. 3.6 is estimated by Eq. (1)

$$F = \frac{2Ee^{(-2r^2/w_0^2)}}{\pi w_0^2} \tag{1}$$

3. Results

3.1 Fluence dependence

In previous studies of sub-100 nm HSFL on titanium, HSFL have been observed at fluences significantly lower than the single-shot ablation threshold $F_{abl} \approx 300$ mJ/cm^2 at $\lambda \approx 800$ nm [19]. For instance, in work of Bonse et al. [12] a value of $F \approx 0.05 - 0.09$ J/cm^2 with the number of pulses $N = 50$ under static irradiation has been reported. While in the work of Golosov et al. [10] a value of $F \approx 0.018$ J/cm^2 at $N \approx 700$ in scanning regime has been reported. The periodicity in both cases was in the same range of $\Lambda \approx 50 - 150$ nm. In the latter case parallel nanoripples were formed inhomogeneously, i.e. along separate stripes, being periodically ordered with distances of about $\Lambda \approx 0.5$ - 0.6 μm.

In our experiments, after irradiation of the titanium film and bulk samples with laser pulses (l = 800 nm, t = 30 fs) in scanning mode with scan speed of 0.2 mm/s ($N \approx 220$), the formation of HSFL was observed in the center of the irradiated region within a narrow fluence range of 30 mJ/cm^2 to 45 mJ/cm^2 (Fig. 1). Above a fluence value of 45 mJ/cm^2 only the formation of LSFL was observed. However on mechanically polished bulk samples, at few regions where the surface is rough, LSFL were observed at fluence values below 45 mJ/cm^2. Moreover, it was found that the quality of nanogratings is much better on mirror-like titanium film sample than on mechanically polished bulk titanium.

#229000 - $15.00 USD Received 4 Dec 2014; revised 30 Jan 2015; accepted 2 Feb 2015; published 25 Feb 2015

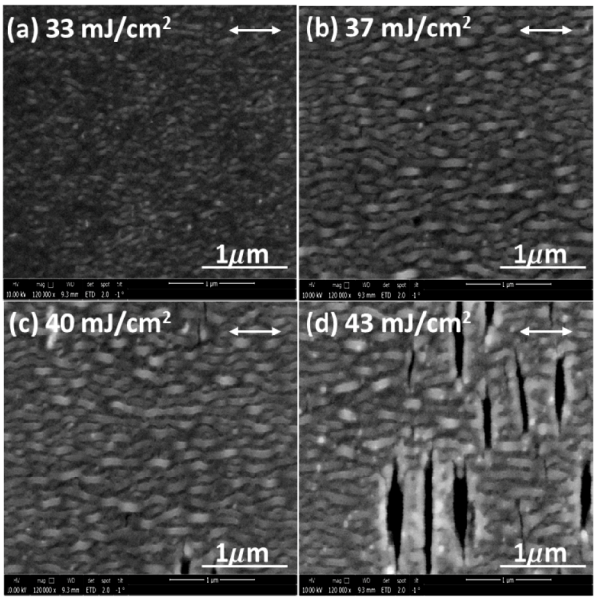

Fig. 1. SEM micrographs of a titanium film surface after irradiation by IR fs-laser pulses (l = 800 nm, t = 30 fs, u = 1 kHz) in the scanning mode with scanning speed of 0.2 mm/s (N ≈220) at various fluence values. The double-headed arrow indicates the direction of the laser beam polarization.

The periodicity of HSFL as a function of fluence on a titanium thin film is shown in Fig. 2(a). Similar values of periodicity and fluence range were observed in a bulk sample. However, in stationary mode, with N = 30, we observed the formation of HSFL at slightly higher fluence values of 60 mJ/cm^2 to 80 mJ/cm^2. The higher threshold value for the formation of HSFL in stationary mode is attributed to a lower number of pulses. Therefore, the so-called incubation law (dependence of threshold values on number of irradiated pulses) [20] is also relevant for HSFL formation. On the other hand, when the titanium film is irradiated by 30 fs pulses using a 50 mm focusing mirror at a scanning speed of 0.6 mm/s (N ≈36), the LSFL periodicity increases from ~460 nm to ~665 nm, as a function of the fluence, (as shown in Fig. 2(b)). It was observed that within a fluence range of ~20 mJ/cm^2, the periodicity increases from a lower value of ~460 nm to a saturation value of ~665 nm. With N ≈36 and fluence values > 120 mJ/cm^2, the film in the central region of irradiation is totally ablated. Compared to HSFL, which exhibit a slow and monotonous rise of periodicity with fluence, LSFL exhibit a step-like increase in periodicity. Similar results of LSFL periodicity dependence on fs-laser fluence have been reported by others [2,12,13,21–23].

#229000 - $15.00 USD Received 4 Dec 2014; revised 30 Jan 2015; accepted 2 Feb 2015; published 25 Feb 2015

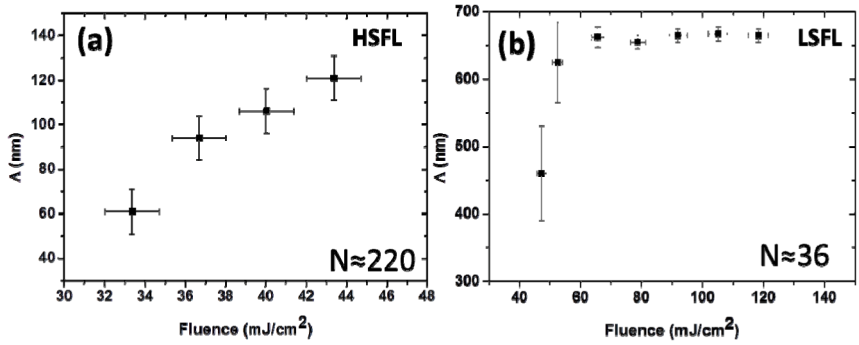

Fig. 2. Dependence of (a) HSFL and (b) LSFL periodicity on Fluence, formed on a titanium film surface when irradiated with t = 30 fs pulses and (a) V = 0.2 mm/s (N ≈220) (b) V = 0.6 mm/s (N ≈36).

3.2 Scanning speed / pulse number dependence

Figure 3 shows SEM micrographs of HSFL on a titanium film formed after irradiation at a fixed fluence of 42 mJ/cm^2 and pulse duration of 30 fs, as a function of scanning speed in the range of 0.2 mm/s – 2.5 mm/s.

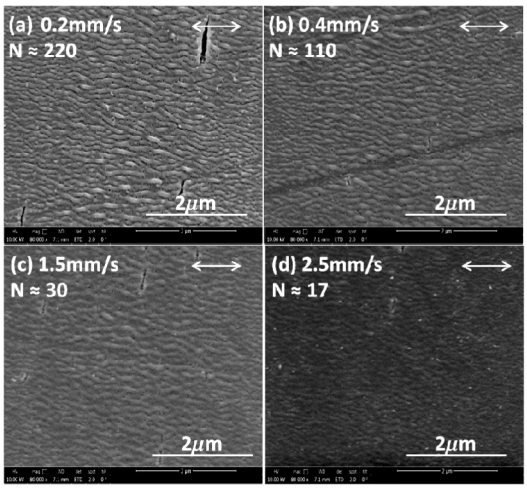

Fig. 3. SEM micrographs of titanium film irradiated by IR fs-laser pulses at F = 42 mJ/cm^2, t = 30 fs, with scan speed (pulse number) variation in the range 0.2 mm/s – 2.5 mm/s (N = 17 - 220). The double-headed arrow indicates the direction of the laser beam polarization.

Figure 4 shows SEM micrographs of LSFL formed on a titanium film surface after irradiation using a 50 mm focal length mirror at a fixed fluence of 65 mJ/cm^2 and a pulse duration of 30 fs as a function of the scanning speed. As can be seen in Fig. 4, at a scanning speed of 0.6 mm/s, the ripples are fully developed and all the material between the ripples is completely removed up to the substrate. At a scanning speed of 0.4 mm/s the central area of irradiation is ablated, and at scanning speeds of 1.5 mm/s and above, the ripples are less pronounced. The dependence of LSFL and HSFL periodicity on scanning speed is shown in Fig. 5.

#229000 - $15.00 USD Received 4 Dec 2014; revised 30 Jan 2015; accepted 2 Feb 2015; published 25 Feb 2015

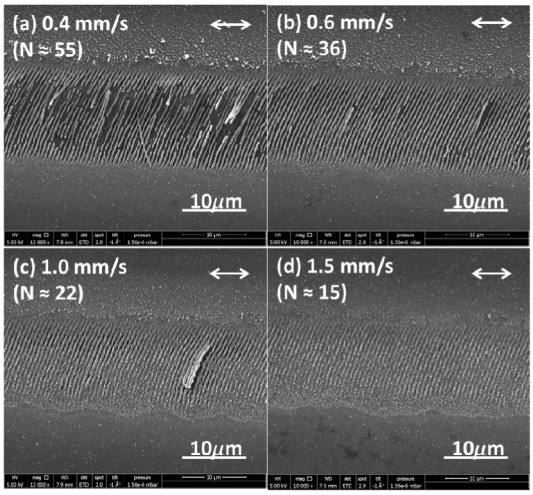

Fig. 4. SEM micrographs of titanium film irradiated by IR fs-laser pulses at F = 65 mJ/cm^2, t = 30 fs, with scanning speed/pulse number variation range 0.4 mm/s – 1.5 mm/s (N = 55 - 15). The double-headed arrow indicates the direction of the laser beam polarization.

The periodicity of HSFL monotonously increases from ~90 nm to ~120 nm when the scanning speed is increased from 0.2 mm/s to 0.8 mm/s (N ≈220 – 55) and is constant in the scanning speed range of 0.8 mm/s – 2.5 mm/s (N ≈55 – 18) (Fig. 5(a)). However this parameter rather strongly affects the quality of HSFL and weakly affects the periodicity. In particular, the best quality of HSFL were achieved at scanning speeds corresponding to N ≈50 - 220 at F = 42 mJ/cm^2. In stationary mode, homogeneous HSFL were achieved at F ≈70 mJ/cm^2 and N ≈10 – 100. At N < 10 the HSFL are weakly ordered and have small height, while at N > 100 they degrade. On the contrary, as shown in Fig. 5(b), the periodicities of LSFL reduce with pulse number in a clearly defined manner, which is consistent with previous reports [5,23,24]. The red curve in Fig. 5(b) is an exponential decay curve fitted to guide the eye. Recently, a new model describing such N-dependent LSFL periodicity in terms of variable surface roughness and SPP scattering has been proposed [23].

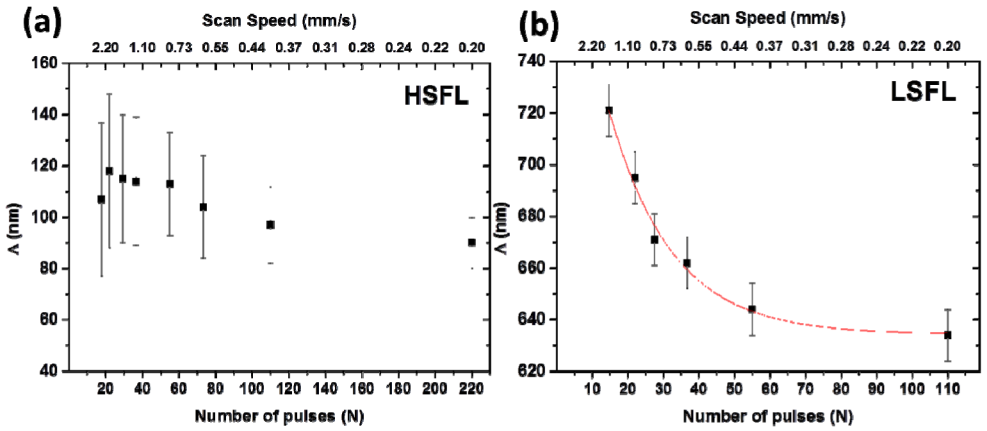

Fig. 5. Dependence of (a) HSFL and (b) LSFL periodicity on scanning speed (pulse number) formed on a titanium film surface when irradiated with t = 30 fs pulses and (a) F = 42 mJ/cm^2 (b) F = 65 mJ/cm^2.

#229000 - $15.00 USD Received 4 Dec 2014; revised 30 Jan 2015; accepted 2 Feb 2015; published 25 Feb 2015

3.3 Pulse duration dependence

In this work, LIPSS parameters were characterized for the first time as a function of pulse widths, providing a novel type of dependence for its characteristics. Figure 6 shows the SEM micrographs of formed HSFL in the central area of irradiation on a titanium film when irradiated with a fixed fluence of F = 42 mJ/cm^2, scanning speed of 0.2 mm/s (N ≈220) and for pulse durations in the range 10 fs – 550 fs. As shown in Fig. 6(f), when the titanium film is irradiated with pulses of 550 fs duration and fluence of 42 mJ/cm^2, the ripples appear isolated and with pulses of duration below 400 fs, they are fully formed.

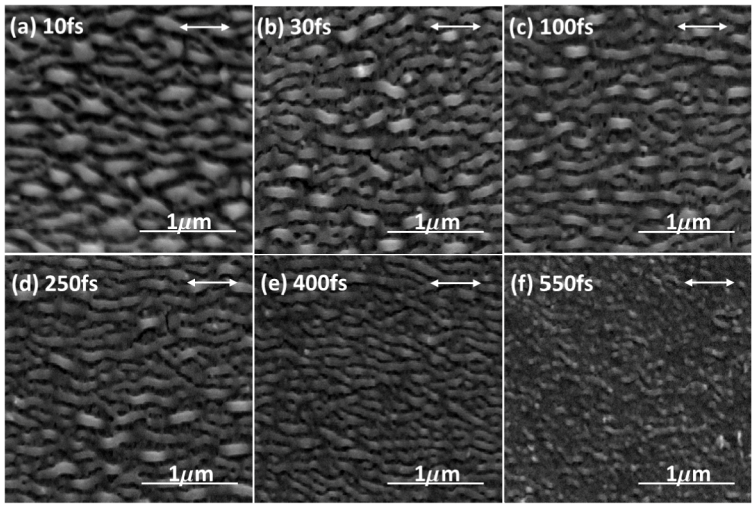

Fig. 6. SEM micrographs of HSFL on titanium film surface when irradiated by IR fs-laser pulses with F ≈42 mJ/cm^2 and scan speed of 0.2 mm/s (N ≈220) of different pulse durations. The double-headed arrow indicates the direction of the laser beam polarization.

It is observed that as the pulse duration is lowered, HSFL formation is more prominent (Fig. 6). We checked the pulse width dependence for bulk titanium sample and the same behavior was observed. Additionally, heights of HSFL on bulk and film samples are in the same range of about 30 nm (Fig. 7). Figure 8 shows the SEM micrographs of LSFL formed in the central area of irradiation on a titanium film when irradiated with fixed fluence of F = 65 mJ/cm^2, scanning speed of 0.6 mm/s (N ≈36) for pulse durations in the range 30 fs – 550 fs.

#229000 - $15.00 USD Received 4 Dec 2014; revised 30 Jan 2015; accepted 2 Feb 2015; published 25 Feb 2015

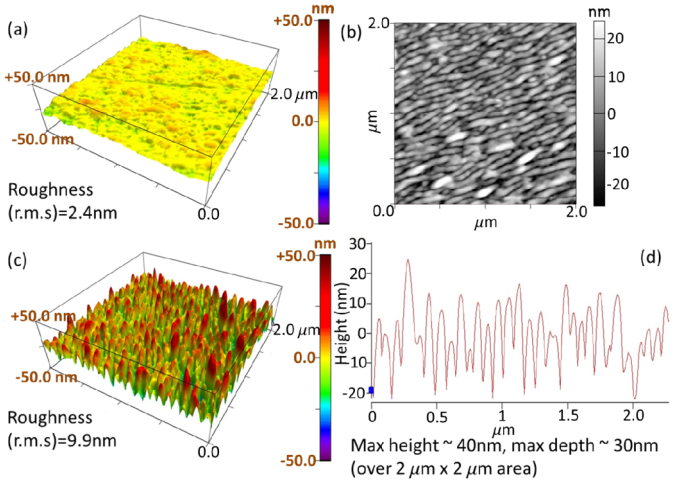

Fig. 7. AFM images of titanium film (a) unexposed area, (b) 2D image of nano-ripples (c) 3D image of nano-ripples (d) Height profile of nano-ripples, after irradiating by IR fs-laser pulses with F = 36 mJ/cm2, t = 30 fs, N ≈220.

The most important finding in this section is the decrease of the HSFL periodicity with pulse duration. This is shown in Fig. 9 for F = 42 mJ/cm^2 and N ≈220, where a relatively moderate decay of the period can be seen. However the periodicity of LSFL was found to be independent on pulse duration. The periodicity of LSFL when irradiated with F = 65 mJ/cm^2 in scanning mode corresponding to N ≈36 pulses is ~660 nm for pulses of duration in the range of 30 – 550 fs. This strongly suggests that the physical processes for formation of these two types of ripples are of different nature.

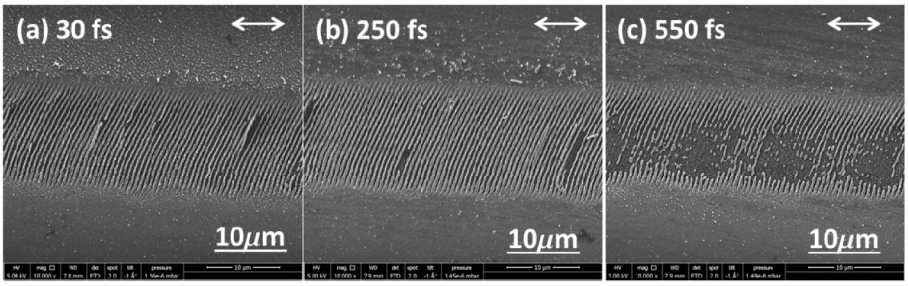

Fig. 8. SEM micrographs of LSFL on titanium film surface when irradiated by IR fs-laser pulses with F ≈65 mJ/cm^2 and scan speed of 0.6 mm/s (N ≈36) at different pulse durations. The double-headed arrow indicates the direction of the laser beam polarization.

#229000 - $15.00 USD Received 4 Dec 2014; revised 30 Jan 2015; accepted 2 Feb 2015; published 25 Feb 2015

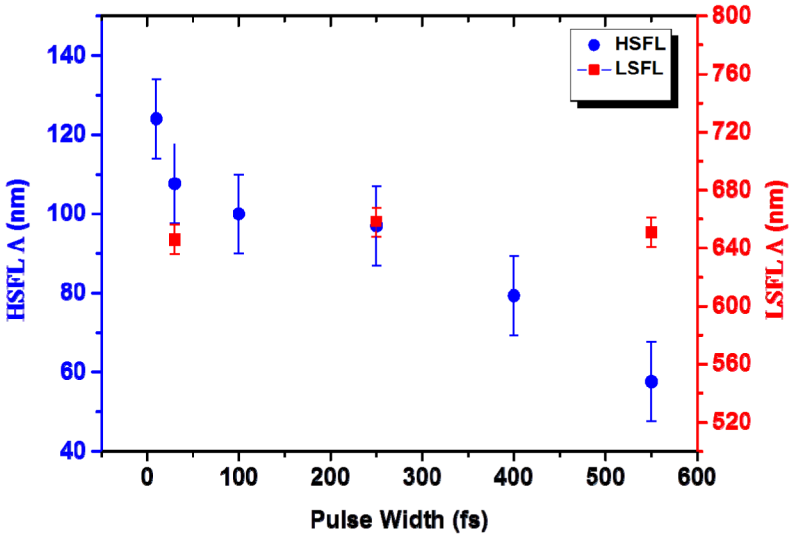

Fig. 9. Periodicity dependence of HSFL (black dots, left axis) and LSFL (blue dots, right axis) on pulse duration on a titanium film surface in scanning mode with: $N \approx 220$, F = 42 mJ/cm^2 for HSFL and N ≈36, F = 65 mJ/cm^2 for LSFL.

The measurements of LSFL topology at different pulse durations revealed strong dependence of their structure quality (Fig. 8) rather than their periodicity (Fig. 9).

3.4 Wavelength dependence

To study the dependence of LSFL and HSFL periodicity on the laser wavelength, we irradiate mirror like titanium film surface by both fundamental (800 nm) and second harmonic (400 nm) of the Ti:Sa laser in the range of F = 30 – 50 mJ/cm^2, and t = 30 – 550 fs in the scanning mode at scanning speeds of 0.2 – 2.5 mm/s. In excellent accordance with the interference model, LSFL exhibit linear dependence of periodicity with wavelength, in agreement with reported experimental observations [3, 25]. When irradiated with a set of chosen experimental parameters (l = 800 nm, F = 48 mJ/cm^2, scanning speed = 0.2 mm/sec (N ≈220), t = 30 fs), the periodicity of LSFL is found to be Λ_{LSFL} ~620 nm. Under similar conditions, when irradiated with 400 nm laser pulses, the periodicity of LSFL was found to be Λ_{LSFL} ~300 nm (Fig. 10(a)). However, the ranges of HSFL periods for both wavelengths (800 nm and 400 nm) was found to be in the same range of 50 – 150 nm, depending on the other laser parameters (Fig. 10(b) and Fig. 1(a)-1(d)). For example, L_{HSFL} ~62 nm, when l = 800 nm, F = 33 mJ/cm^2, N ≈220, t ~30 fs, and L_{HSFL} ~65 nm when l = 400 nm, F = 25 mJ/cm^2, N ≈220, t ~30 fs. This is in striking contrast with experimental observations in [16], demonstrating a monotonous increase of HSFL periodicity with laser wavelength (l ≈1.4 – 2.2 mm). However in the experiments in [16] the photoexcitation conditions were not kept identical over the spectral range.

#229000 - $15.00 USD Received 4 Dec 2014; revised 30 Jan 2015; accepted 2 Feb 2015; published 25 Feb 2015

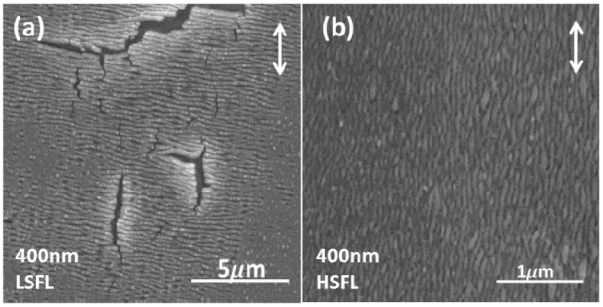

Fig. 10. SEM micrographs of (a) LSFL and (b) HSFL formed on a titanium film surface after irradiation with l = 400 nm, F = 25 mJ/cm^2, N ≈220, t ~30 fs pulses. The double-headed arrow indicates the direction of the laser beam polarization.

3.5 Polarization dependence

The comparison of LSFL and HSFL ridges orientation exhibit a similar picture at different wavelengths, fluences, pulse durations, shots numbers and thickness of sample. LSFL and HSFL are always perpendicular to each other. In general, HSFL are always parallel to the laser polarization (Fig. 11) (see also Table 1 in [12]), while LSFL are perpendicular to the laser polarization (Fig. 1(d), Fig. 4, and Fig. 8) as usually observed [26].

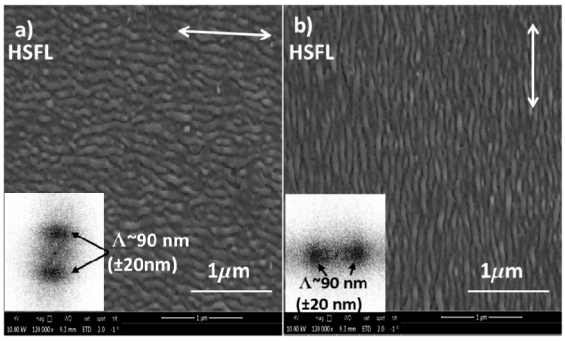

Fig. 11. SEM micrographs of HSFL formed on a titanium film after irradiation with IR laser pulses with F = 36 mJ/cm^2, N ≈220, t = 30 fs. The double-headed arrow indicates the direction of the laser beam polarization. The corresponding 2D Fourier transformations of SEM micrographs are shown in the insets.

3.6 Surface-roughness dependence

In order to reveal possible correlation between LSFL and HSFL we also compared titanium surfaces with different roughness quality. In Fig. 7(a) the roughness of initial surface of mirror-like Ti film is presented, indicating absence of any nano-tranches. Figure 12(d) shows SEM micrograph of the initial roughness of bulk titanium surface. Indeed, in case of mirror-like surface quality only homogeneously distributed HSFL are formed at any fluence values in agreement with some previous studies [11]. However, presence of initial tranches on the bulk titanium surface leads to coexistence of LSFL and HSFL at near-threshold fluences F ≈60 mJ/cm^2 at N = 70 (Figs. 12(a) and 12(b)) in agreement with the other previous studies [9, 10]. At higher fluences of F ≈80 mJ/cm^2 at N = 20 the HSFL fill the irradiated area homogeneously and almost independent of the nanoroughness (Fig. 12(c)). On the other hand, as mentioned in Sec. 3.1, the threshold fluence for formation of LSFL is lower on rough titanium surface compared to mirror like titanium surface, which is in good agreement

#229000 - $15.00 USD Received 4 Dec 2014; revised 30 Jan 2015; accepted 2 Feb 2015; published 25 Feb 2015

with a previous study [27]. It should be noted that the periodicity of LSFL is about half near the threshold and are referred to as 'fine ripples' in [27].

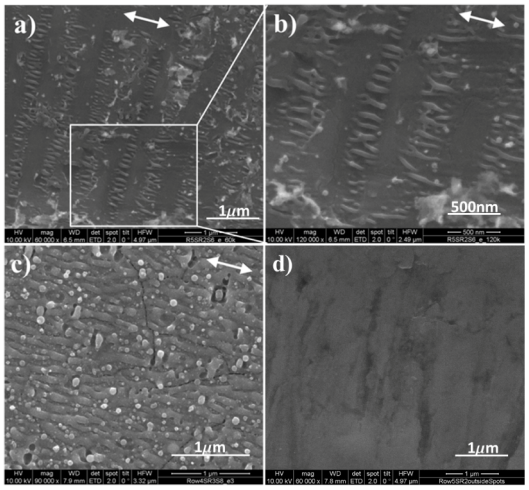

Fig. 12. SEM micrographs of HSFL on bulk titanium surface when irradiated by 30 fs IR laser pulses with (a, b) F ≈60 mJ/cm^2, N = 70 (c) F ≈80 mJ/cm^2, N = 20 (d) un-exposed area. The double-headed arrow indicates the direction of the laser beam polarization.

4. Discussion

In order to provide a systematic, qualitative overview of these experimental results, we summarize the observations in Table 1, where one can see that LSFL and sub-100-nm HSFL generated on titanium surface irradiated in air environment exhibit an opposite trend with varying basic laser parameters. These laser parameters were proven to be of major significance in the process of LSFL formation. In particular, the interference model implies linear explicit dependence on the laser wavelength [7] with some nonlinear influence arising from dispersion of the dielectric function and the number of shots via grating coupling [5]. However, HSFL are much less dependent on these two parameters as LSFL does.

Table 1. Main dependences of LIPPS period on laser parameters.

Laser Parameters / Structures	Wavelength	Fluence	Shots number	Pulse duration
LSFL (⊥ to polarization)	Dependent	Dependent	Dependent	Not dependent
HSFL (‖ to polarization)	Not dependent	Dependent	Weakly dependent	Dependent

In spite of the fact that generally both LSFL and HSFL exhibit a fluence-dependent periodicity, the characters of the dependencies are quite different. According to the literature data, the periods of LSFL are changed slowly at high fluences [2,22] and dropped by two times near the threshold of their formation [4,22,23], which is in good agreement with our data for LSFL. All these variations of LSFL periodicity occur in the fluence range of 0.04 – 0.12 J/cm^2 (Fig. 2(b)), comparing to LSFL generation range of 0.08 – 0.35 J/cm^2 reported in [12], where in the latter case the lower fluence limit represents minute spallation and higher fluence limit represents deep fragmentation ablation thresholds for titanium, according to the constant spallation and linear fragmentation yields of atomic emission recorded in our optical emission studies of ablative plumes [28] and previous studies [19]. In contrast to LSFL, HSFL exhibit significant dependency on laser fluence (Fig. 2) below the spallative ablation

#229000 - $15.00 USD Received 4 Dec 2014; revised 30 Jan 2015; accepted 2 Feb 2015; published 25 Feb 2015

threshold [28], where intense sub-surface cavitation occurs [10, 11]. Also, smaller but clear dependence on pulse duration of HSFL has been found, whereas LSFL periodicity does not depend on pulse duration. Thus, bearing in mind that intensity is $I = F/\tau$, the dependence of the periodicity on intensity for HSFL is even more rapid as compared with LSFL. In particular, the fitting of $\Lambda(F)$ and $\Lambda(\tau)$ dependencies are $\Lambda \sim F^{1.5 \pm 0.6}$ (Fig. 2(a)) and $\Lambda \sim \tau^{0.2 \pm 0.1}$ (Fig. 9) gives nonlinear dependence $\Lambda \sim I^{1.7 \pm 0.7}$. The non-linear character of this dependence apparently depends on fs-laser energy deposition and electron dynamic details, which have to be understood yet for titanium, using, e.g., the pulse width dependency of spallation and fragmentation ablation thresholds [29].

An additional problem for the interference model arises when one needs to explain why LSFL and HSFL with crossed orientations can co-exist in the same surface area. Such cross oriented structures, which are both LSFL, have been observed in double pulse experiments also [30,31]. According to the interference model [7,8,13] LIPSS with parallel orientation to the laser polarization requires real part of the photo-excited dielectric function of the metal, $\Re e(\varepsilon_m) > -1$. Hence, in air environment with dielectric function ε_d (where $\Re e(\varepsilon_d) \approx 1$) only separate formation of LSFL at $\Re e(\varepsilon_m) < -1$ and HSFL at $\Re e(\varepsilon) > -1$ is expected [7,8,13,32,33]. However, according to the experimental results of our present and previous studies [10,11], regimes where LSFL and HSFL co-exist were revealed. Moreover, very recently another SPP-based model of HSFL formation was reported [16] where nanoripples are created on a titanium foil by exploiting laser induced oxidation and *in situ* generation of third harmonic of Ti:sapphire laser operating at wavelengths in the range of 1.4 – 2.2 mm. The observed HSFL period which is in the order of one tenth of the irradiating laser wavelengths was explained by excitation of short-wavelength SPP by the generated third-harmonic-radiation at the oxidized interface with much higher refractive index of titanium oxides. However, the laser-induced 10-nm thick oxide layer can affect only wavelengths of sub-wavelength longitudinal surface electromagnetic waves (surface plasmons) with $\Re e(\varepsilon_m) \to -\Re e(\varepsilon_d)$, which are strongly localized in the metal and dielectric near the interface within the corresponding penetration depths d and D given by Eqs. (2,3, comparing to presumably transverse near-wavelength surface polaritons at $\Re e(\varepsilon_m) \ll -\Re e(\varepsilon_d)$, which usually exhibit sub-micron depths in the boundary dielectric medium [33].

$$d \approx \frac{\lambda}{2\pi}\sqrt{\frac{\varepsilon_m + \varepsilon_d}{\varepsilon_m^2}}, \tag{2}$$

$$D \approx \frac{\lambda}{2\pi}\sqrt{\frac{\varepsilon_m + \varepsilon_d}{\varepsilon_d^2}}. \tag{3}$$

Moreover, the ultimate wavelength of surface plasmons in corresponding surface plasmon resonance, given by the condition $\Re e(\varepsilon_m) = -\Re e(\varepsilon_d))$, is not directly scalable with the incident laser wavelength, i.e., is hardly affected by the third-harmonic radiation [34].

Also, we have mentioned in the introduction, that HSFL on Ti have been previously observed as two different types: (i) combination of LSFL and HSFL [10]; or (ii) only HSFL [12]. Our detailed analysis of fluence dependence reveals both these types at slightly different conditions. In particular, under irradiation of bulk Ti by $N \approx 30$ laser pulses with duration of $\tau \approx 30$ fs and fluence of $F < 60$ mJ/cm^2 the HSFL appear only inhomogeneously (Figs. 12(a) and 12(b)). The periodicity of HSFL in this case is about $\Lambda \approx 70$ nm and width of each stripe is about 200 nm. The periodicity is stable in this range of fluences, but increases rapidly up to $\Lambda \approx 140$ nm at higher fluence $F \approx 80$ mJ/cm^2, where spallative ablation starts to destroy HSFL (see also [12]). The increased values of period correspond to homogeneously distributed nanoripples (Fig. 12(c)). Importantly, we did not observed any inhomogeneous HSFL formation on mirror-like Ti film, where only homogeneous HSFL formation was observed.

#229000 - $15.00 USD Received 4 Dec 2014; revised 30 Jan 2015; accepted 2 Feb 2015; published 25 Feb 2015

Such a strong dependences of HSFL type on surface quality can be explained in terms of the interference model of LSFL formation. In case of rough surface with a lot of initial trenches ("sources" of light scattering) (Fig. 12(d)), they provide SPP excitation and interference pattern formation around themselves. These patterns usually are stable from pulse to pulse, if the local fluence in the interference maxima is not too high to produce new deep trenches, i.e. when it is lower than the corresponding LSFL formation threshold. In this case the laser energy is absorbed many times along narrow separated stripes. The opposite is true when the initial surface is smooth with nano-roughness growing randomly from pulse to pulse, which does not provide fixed interference pattern, resulting in emerging of maxima on new places after each shot. Therefore, a surface without single "sources" for SPP cannot exhibit formation of inhomogeneous HSFL.

One possible mechanism for the formation of sub-100-nm HSFL structures on titanium surface under femtosecond pulses irradiation can be the previously proposed cavitation-instability mechanism [9, 10] which is based on intense reversible and irreversible pre-spallation sub-surface boiling (thermally-induced cavitation). This results in relief restoration at the sub-threshold fluences and surface swallowing at fluences approaching the corresponding spallation threshold [35,36]. It predicts formation of sub-surface nanobubbles in the molten surface layer along each narrow and long interference surface stripe formed via interference of the incoming light with excited SPP. At higher fs-laser fluences, exceeding the ripple formation threshold, such sub-surface nanobubbles are merged together into a longitudinal vapor nanocavity along the stripe, then expelling the top liquid overlayer and making a spallative ripple trench. At lower fluences such nanobubbles can make longitudinal self-organized sequences of tightly spaced, separated closed nanovoids (nanospikes at sub-threshold fluences [10]) or separated open nanovoids (nanopores at near-threshold fluences [10,37]) through their collective repulsive interaction [38], which finally remain frozen in the quasi-regular structures. Indeed, in such regime, surface is heated along narrow stripes resulting in formation of LSFL at local fluences higher than ablation threshold or HSFL at fluences lower than the ablation threshold [10,11].

Our present experiments support this mechanism. At higher fluences ($F > 80$ mJ/cm^2), HSFL represent aligned open nanovoids (Fig. 13). At higher exposures open nanovoids are merged into trenches, forming LSFL. The same broken voids were noticed for HSFL on aluminum [10] indicating the universal character of this mechanism. Indeed, sub-surface cavitation under ultrashort laser irradiation is the universal effect for different materials [39,40].

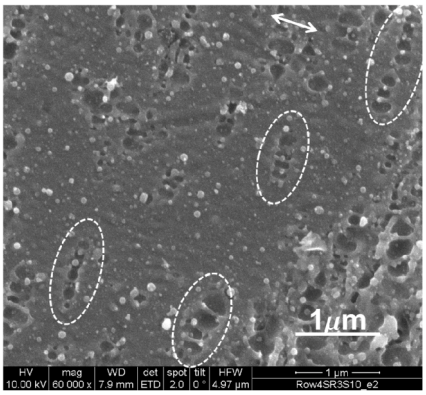

Fig. 13. SEM micrographs of HSFL on bulk titanium surface when irradiated by 30 fs IR laser pulses with $F \approx 80$ mJ/cm^2, $N = 5$. The double-headed arrow indicates the direction of the laser beam polarization.

#229000 - $15.00 USD Received 4 Dec 2014; revised 30 Jan 2015; accepted 2 Feb 2015; published 25 Feb 2015

5. Summary and conclusions

In this work the near wavelength structures (LSFL), and sub-100-nm structures (HSFL) were made on a titanium surface by irradiating the surface with linearly polarized femtosecond (fs) laser pulses in air environment. In scanning mode with scanning speed of 0.2 mm/s (N ≈220), and t = 30 fs, HSFL form parallel to the laser polarization within a narrow fluence range of 30 mJ/cm^2 to 45 mJ/cm^2, and the periodicity increases with fluence. With number of pulses, the periodicity of HSFL do not show a clear trend, but the periodicity of LSFL reduces exponentially. The periodicities of both types of LIPSS demonstrate opposite pulse duration and wavelength dependencies, which suggest their origins are different and cannot be explained by interference model developed for LSFL.

Acknowledgments

This work was supported by the Österreichische Forschungsfödergesellschaft (FFG) (Project 834325) and by the Government of the Russian Federation (Grant 074-U01) through ITMO Post-Doctoral Fellowship for S.V.Makarov. The SEM measurements were carried out using facilities at the University Service Centre for Transmission Electron Microscopy, Vienna University of Technology, Austria. We thank Dr. Yuyu Wang for the help in imaging the samples by AFM.

#229000 - $15.00 USD Received 4 Dec 2014; revised 30 Jan 2015; accepted 2 Feb 2015; published 25 Feb 2015